Catalysts **2015**, *5*, 1152-1166; doi:10.3390/catal5031152

OPEN ACCESS

catalysts

ISSN 2073-4344

www.mdpi.com/journal/catalysts

Article

Continuous Catalytic Hydrodeoxygenation of Guaiacol over Pt/SiO_2 and Pt/H-MFI-90

Melanie Hellinger [1,2], Sina Baier [1], Peter Mølgaard Mortensen [3], Wolfgang Kleist [1,2], Anker Degn Jensen [3] and Jan-Dierk Grunwaldt [1,2,*]

[1] Institute for Chemical Technology and Polymer Chemistry (ITCP), Karlsruhe Institute of Technology, Karlsruhe D-76128, Germany; E-Mails: melanie_h@online.de (M.H.); sina.baier@kit.edu (S.B.); wolfgang.kleist@kit.edu (W.K.)

[2] Institute of Catalysis Research and Technology (IKFT), Karlsruhe Institute of Technology, Eggenstein-Leopoldshafen D-76344, Germany

[3] Department of Chemical and Biochemical Engineering, Søltofts Plads, Building 229, Technical University of Denmark, Lyngby DK-2800, Denmark; E-Mails: pmor@topsoe.dk (P.M.M.); aj@kt.dtu.dk (A.D.J.)

* Author to whom correspondence should be addressed; E-Mail: grunwaldt@kit.edu; Tel.: +49-721-608-42120; Fax: +49-721-608-44820.

Academic Editor: Keith Hohn

Received: 28 April 2015 / Accepted: 19 June 2015 / Published: 3 July 2015

Abstract: Hydrodeoxygenation of guaiacol in the presence of 1-octanol was studied in a fixed-bed reactor under mild conditions (50–250 °C) over platinum particles supported on silica (Pt/SiO_2) and a zeolite with framework type MFI at a Si/Al-ratio of 45 (Pt/H-MFI-90). The deoxygenation selectivity strongly depended on the support and the temperature. Both guaiacol and octanol were rapidly deoxygenated in the presence of hydrogen over Pt/H-MFI-90 at 250 °C to cyclohexane and octane, respectively. In contrast, Pt/SiO_2 mostly showed hydrogenation, but hardly any deoxygenation activity. The acidic sites of the MFI-90 support lead to improved deoxygenation performance at the mild temperature conditions of this study. Significant conversions under reaction conditions applied already occurred at temperatures of 200 °C. However, during long-term stability tests, the Pt/H-MFI-90 catalyst deactivated after more than 30 h, probably due to carbon deposition, whereas Pt/SiO_2 was more stable. The catalytic activity of the zeolite catalyst could only partly be regained by calcination in air, as some of the acidic sites were lost.

Keywords: continuous process; guaiacol; hydrodeoxygenation; 1-octanol; Pt catalysts; zeolites; bio-oil upgrading

1. Introduction

Biomass is the world's largest sustainable carbon-based energy source. Hence, biomass-derived molecules are attractive raw materials for fuels and chemicals [1]. Currently, one of the most promising routes is the combination of flash pyrolysis and hydrodeoxygenation [2–5]. In flash pyrolysis, biomass is rapidly heated up to 450–500 °C, and the vapors are subsequently quenched. Thereby, the energy density of the biomass is increased. The resulting bio-oil, which contains a variety of oxygen-rich compounds, is chemically unstable and undergoes oligomerization and polymerization reactions over time and temperature. One of the reasons is the high content of phenolic compounds originating from the lignin part of the biomass [6]. Therefore, the removal of these oxygen functions using, e.g., hydrodeoxygenation is required, resulting in sustainable chemicals and fuels [2,7].

During hydrodeoxygenation of bio-oil or specific biomass-derived model compounds, hydrogen is consumed as in hydrodesulfurization to remove heteroatoms. Various catalytic systems have been reported in the literature [2,7]. Among the most prominent classes of catalysts are CoMo- and NiMo-based hydrodesulfurization catalysts and Ni-based systems [8–10]. Although these catalysts are attractive, as they are rather inexpensive, they often exhibit a lower activity than supported noble metal catalysts [11–14]. The former are, however, known to be more stable in the presence of sulfur impurities and have, thus, been studied in continuous operation. However, these catalysts typically desulfurize with time-on-stream, leading to sulfur enrichment of the products, as well as catalyst deactivation [15,16]. The group of Gates [17–20] reported extensive hydrodeoxygenation studies of guaiacol over 1 wt. % Pt/Al_2O_3 and 1 wt. % Pt/MgO. Three major reaction types were observed: hydrogenolysis and hydrogenation over the noble metal and transalkylation probably promoted by the support. Catalyst deactivation occurred faster at lower space velocities and higher temperatures (250–350 °C). Hydrodeoxygenation was preferred at higher temperatures and increased hydrogen pressure.

Alternatively, zeolites have been investigated for the upgrading of biomass-derived oxygenates and phenolic compounds [2,7]. They offer sufficient thermal stability, high specific surface area and a high acidity compared to metal oxides. Studies over the zeolite H-ZSM-5 were performed both on model compounds [21,22] and pyrolysis oil [23–25], even at atmospheric pressure [7,23]. Gayubo *et al.* [21] studied the transformation of alcohols and phenols over H-ZSM-5 between 200 and 450 °C. In the first step, dehydration of the alcohol took place, while a further transformation into hydrocarbons occurred in subsequent reaction steps. The conversion to butenes and propenes was smaller for phenol, and hardly any cracking products were found for guaiacol (dissolved in toluene). Furthermore, carbon deposition was observed, and temperatures above 400 °C were required. Vitolo *et al.* [25] reported not only on the transformation of pyrolysis oil, but also on catalyst regeneration over ZSM-5, which could at least to a certain extent be achieved by calcination in air. Noble metal particles supported and other active metals on zeolites were used as an alternative [26–29] Thereby, also ring-opening and

corresponding hydrogenated intermediates were observed at 350–450 °C and 20–50 bar [28]. As zeolites alone suffer from carbon deposition and deactivation, the addition of noble metals supported on zeolites appeared beneficial [26,28]. Furthermore, gallium-modified beta zeolites were reported at 400–450 °C and 1 bar of H_2. *m*-Cresol was mainly transformed into aromatic products, like toluene, benzene and xylene [29]. Higher hydrogen pressures were beneficial for catalyst performance and stability. Hence, the study of noble metal catalysts supported on zeolites appears attractive. In a recent screening work, we extended this approach and studied the conversion of guaiacol over several supported platinum catalysts in batch operation under mild conditions. Among those, Pt/SiO_2 and Pt/H-MFI-90 appeared most attractive in a temperature range up to 200 °C [30]. In this previous study [30], as well as studies by Faglioni and Goddard [31] and Mortensen *et al.* [32], hydrogenation followed by dehydration was found to be the preferred pathway at these lower reaction temperatures ($T \leq 250$ °C).

To exploit these mild reaction conditions in more detail, we report in the present study on the conversion of guaiacol in 1-octanol over Pt/SiO_2 and Pt/H-MFI-90 in a continuous flow setup at mild reaction temperatures ($T \leq 250$ °C). 1-Octanol was used as the solvent, because it is able to form a single-phase mixture with guaiacol [32]. In addition, it represents an alcoholic fraction of bio-oils, even though 1-octanol is not present in bio-oils. Compared to batch reactor studies, the continuous reactor offered the possibility to study the long-term stability of selected catalysts (see also [32,33]), which is crucial for a full evaluation of its performance. Furthermore, variations of the reaction conditions, studies on the kinetics or regeneration experiments are easier to perform in a continuous reactor. In particular, the stability of the catalysts and the influence of the reaction temperature (50–250 °C) were investigated in detail using long-term studies and recycling experiments, as well as various catalyst characterization methods before and after the experiments.

2. Results and Discussions

2.1. Catalyst Characterization

The specific surface areas (S_{BET}) of the catalysts and the supports are summarized in Table 1. For the silica and H-MFI-90-supported catalysts, similar surface areas at different loading were obtained; a higher specific surface area was found for the zeolite-supported catalyst. The values were almost identical to the pure support material.

Table 1. Textural properties of the supports and the prepared catalysts (for details on XRD analysis and ammonia adsorption, *cf.* Figures S1 and S2 in the electronic support information, respectively).

Materials	Pt Loading	S_{BET}	NH_3 Adsorption (µmol/g)		Particle Size
	(%)	(m^2/g)	Weak	Strong	(nm)
SiO_2	0	197	4	-	-
1 wt. % Pt/SiO_2	1	187	27	-	1.3 [b]
5 wt. % Pt/SiO_2	5	185	125	-	2.1 [a]
H-MFI-90	0	417	352	254	-
1 wt. % Pt/H-MFI-90	1	414	415	286	1.1 [b]

[a] Crystallite size estimated from XRD (Scherrer equation); [b] particle size estimated from STEM images.

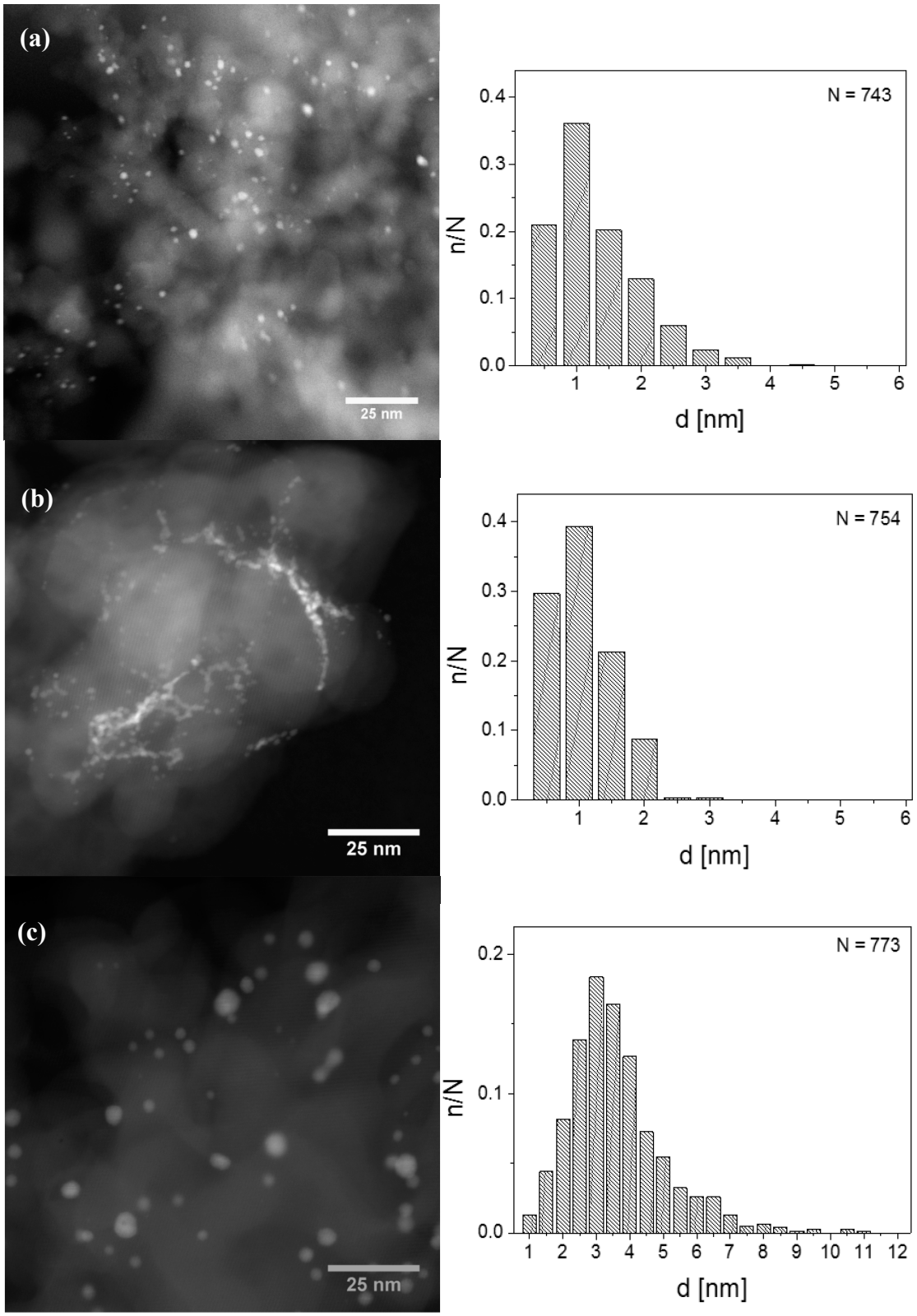

Figure 1. STEM images and particle size distribution of 1 wt. % Pt/SiO_2 (**a**); 1 wt. % Pt/H-MFI-90 (**b**); and 1 wt. % Pt/H-MFI-90 after the catalytic measurement at 250 °C (**c**).

Furthermore, the weak and strong acidic sites based on NH_3 desorption temperature are given in Table 1. H-MFI-90 was significantly more acidic, compared to SiO_2. For the catalysts with a Pt loading of 1 wt. %, no Pt reflections were observed in the XRD patterns (see also [30]). The noble

metal particles seem to be highly dispersed and very small (Figure S1). In contrast, a characteristic reflection of platinum oxide was observed at 2θ = 34.2° for the calcined catalyst with 5 wt. % Pt/SiO_2. After reduction, reflections of metallic Pt appeared at 40.1°, 46.6° and 67.7° (Figure S1). The crystallite sizes estimated by the Scherrer equation were around 2 nm for the calcined sample and between 2 and 5 nm for the reduced one.

To gain more information about the particle size distribution, the prepared oxide catalysts were investigated by STEM (Figure 1). For the fresh catalysts in both cases, small Pt particles were observed for 1 wt. % Pt/SiO_2 and 1 wt. % Pt/H-MFI-90 with an average diameter of 1.3 ± 0.7 nm and 1.1 ± 0.5 nm, respectively. As expected from the XRD measurements, the silica-supported catalysts showed small and highly-dispersed Pt particles in a range from 0.5–4.5 nm (Figure 1a). The comparison of the particle size distribution of the calcined 1 wt. % Pt/SiO_2 catalyst and the catalyst after reaction at 250 °C shows a significant increase of the particle size (see the following section). Particle sintering was also observed after reduction by XRD for 1 wt. % Pt/SiO_2 and especially 5 wt. % Pt/SiO_2 (Figure S1).

While homogeneously-distributed small Pt particles were visible for the fresh silica-supported catalyst, the particles on the fresh H-MFI-supported catalyst were less homogeneously deposited. For 1 wt. % Pt/H-MFI-90, the particles are located on the boundary layer of H-MFI-90 (Figure 1b). The particles were in the range between 0.5 and 3 nm and, therefore, had a slightly smaller average particle size than on the silica-supported catalyst.

2.2. Comparison of the Catalytic Performance and Stability of Pt/SiO_2 and Pt/H-MFI-90

The performance and stability of the three different catalysts were studied in the hydrodeoxygenation of guaiacol and 1-octanol for both 5 wt. % Pt/SiO_2 and 1 wt. % Pt/SiO_2 (Figure 2), as well as for 1 wt. % Pt/MFI-90 (Figure 3). Tables S1–S7 summarize the catalytic data complementary to those given in the manuscript figures as the conversion and yields of the corresponding products in tabular format.

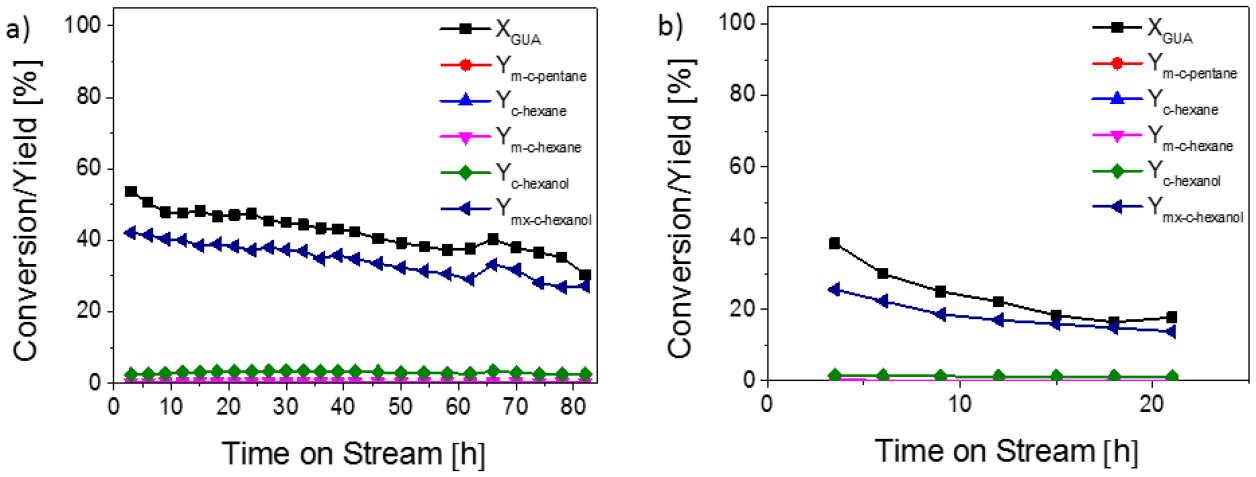

Figure 2. Conversion of guaiacol over (**a**) 5 wt. % Pt/SiO_2 and (**b**) 1 wt. % Pt/SiO_2 (conditions: 0.3 mL/min 5% GUA in 1-octanol, 500 mL/min 80% H_2 in N_2, T = 250 °C, p = 100 bar, 1 g catalyst; GUA = guaiacol, m = methyl, mx = methoxy, c = cyclo).

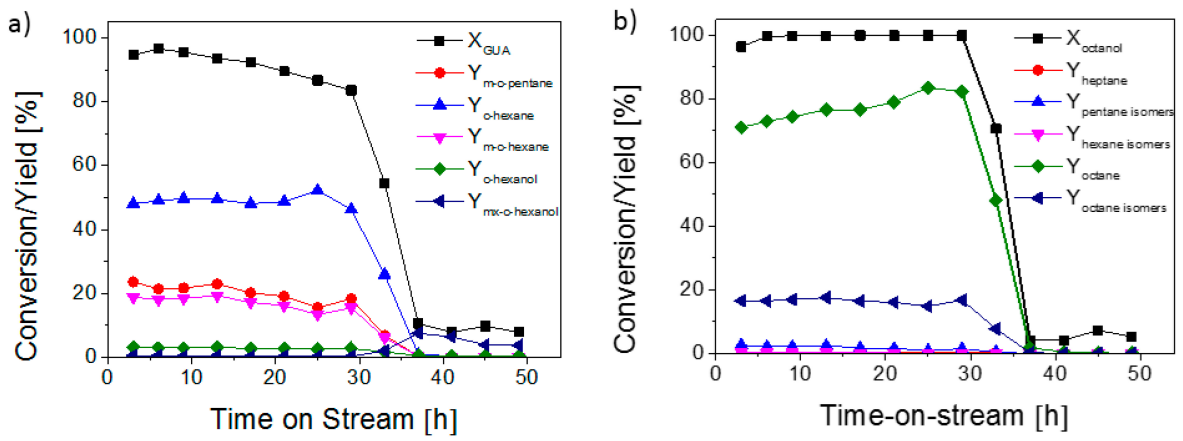

Figure 3. Conversion of (**a**) guaiacol and (**b**) 1-octanol over 1 wt. % Pt/H-MFI-90 as a function of time-on-stream (conditions: 0.3 mL/min 5% GUA in 1-octanol, 500 mL/min 80% H_2/N_2, T = 250 °C, p = 100 bar, 1 g catalyst; GUA = guaiacol, m = methyl, mx = methoxy, c = cyclo).

Using the silica-supported catalysts, 1-octanol was not deoxygenated. Instead, only hydrogenation of guaiacol to methoxycyclohexanol occurred, and a decreasing guaiacol conversion was observed over time-on-stream. With the 5 wt. % Pt/SiO_2 catalyst, the highest conversion was 53%, which decreased to 32% after 82 h (Figure 2a). For 1 wt. % Pt/SiO_2, the conversion decreased from 38% down to 18% after 21 h (Figure 2b). Because of the negligible acidity of the support material (Table 1), only low amounts of cyclohexane were formed during the reaction. Due to the higher Pt-loading, for the catalyst with 5 wt. % platinum, both a higher conversion of guaiacol and yield of methoxycyclohexanol were found, compared to 1 wt. % Pt/SiO_2.

For the 1 wt. % Pt/H-MFI-90, a different catalytic behavior was observed, compared to the silica-supported catalysts. With the zeolite catalyst, both guaiacol and 1-octanol were converted. Nearly full conversion of 1-octanol to octane (71%) and its isomers (17%) was found, with pentanes being detected as minor by-products (<3%) (Figure 3b). For guaiacol, also complete conversion to cyclohexane (48%), methylcyclohexane (19%), methylcyclopentane (24%) and low amounts of cyclohexanol (3%) (Figure 3a) was obtained. In accordance with the higher acidity, 1 wt. % Pt/H-MFI-90 showed increased hydrodeoxygenation ability, but deactivated already after 33 h of time-on-stream. Methoxycyclohexanol appeared as a product indicating that deoxygenation was more affected than hydrogenation. After 37 h time-on-stream, only low amounts of guaiacol and 1-octanol were converted. Note that the deactivation at 250 °C occurred first slowly and then abruptly. At lower temperatures (Figure S3), deactivation occurred slowly over the whole time. At higher temperatures, initially, the conversion was high, and the catalyst bed was only partly used, leading probably to a moving deactivation front through the reactor, indicating that the active sites of the catalyst are blocked.

Temperature programmed oxidation (TPO) of the spent 1 wt. % Pt/H-MFI-90 catalyst (Figure 4a) revealed 7 wt. % of coke on the catalyst, which could be oxidized between 300 and 400 °C. This is in accordance with literature reports [11,25,34]. Obviously, with decreasing temperature, lower carbon deposition was found. One suggestion could be that a shorter reaction time leads to a smaller amount of carbon. However, by comparison of the experiments at 250 and 200 °C, which have a similar

reaction time of 50 h time-on-stream, it can be concluded that the temperature, and not the reaction time, is the determining factor for the carbon deposition. For Pt/H-MFI-90, higher coke concentrations were found than for the silica-supported catalysts (Table 2). 5 wt. % Pt/SiO_2 has a longer reaction time-on-stream and a lower carbon deposition; this leads to the suggestion that the higher acidity of H-MFI 90 is responsible for the higher carbon deposition, which has also been observed on other zeolite-based catalysts (see [12,22]).

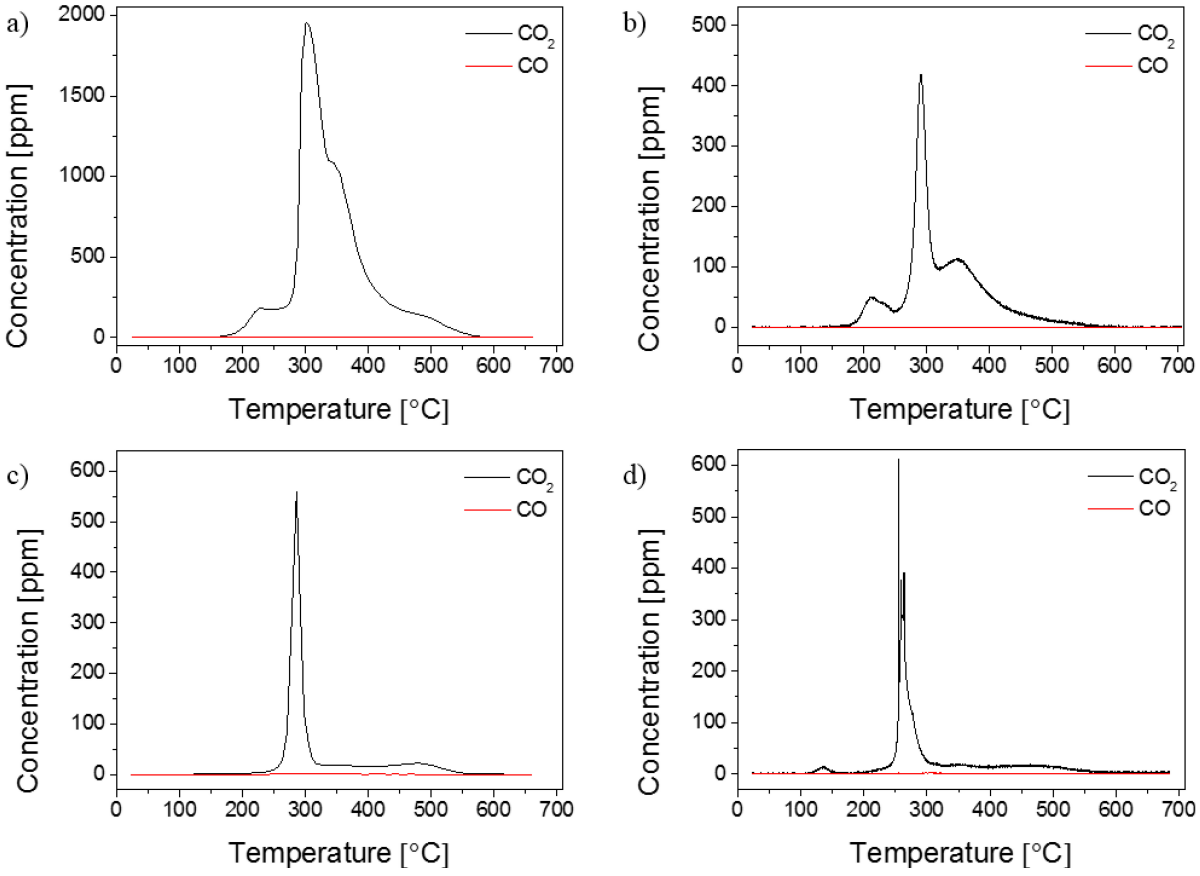

Figure 4. Results of the temperature programmed oxidation of (**a**) 1 wt.% Pt/H-MFI-90, (**b**) 1 wt. % Pt/H-MFI-90$_{rec.}$, (**c**) 5 wt. % Pt/SiO_2 and (**d**) 1 wt. % Pt/SiO_2 after the catalytic measurement at 250 °C (conditions: 1 L/min 10% O_2 in N_2, T = 25–700 °C, 5 K/min, (**a**) 100 mg; (**b**–**d**) 10 mg catalyst).

Table 2. Catalyst properties after the catalytic measurements at 150, 200 and 250 °C.

Catalysts	Temperature	Carbon Deposition	Particle Size	NH_3 Adsorption (µmol/g)	
	(°C)	(%)	(nm)	Weak	Strong
1 wt. % Pt/SiO_2	250	5.0	4–10 [a]	9	13
5 wt. % Pt/SiO_2	250	4.1	7–8 [a]	9	-
1 wt. % Pt/H-MFI-90	250	7.0	-	-	-
	250$_{rec.}$	7.5	3.5	236	71
	200	5.5	-	433	98
	150	2.8	-	303	214

[a] Estimated from XRD patterns by the Scherrer equation from the different reflections.

Besides coke deposition, also sintering of the Pt particles may lead to deactivation [34]. Both STEM (Figure 1) and XRD (Figure S1) indicate sintering (Table 2). In the case of Pt/H-MFI-90, sintering was less pronounced than for the SiO_2-supported catalysts. This may be due to the higher surface area of the zeolite or the inhibition by the size of the pores, and thus, coke deposition may be the main deactivation pathway on Pt/H-MFI-90 [34].

In contrast to this work, most studies on Pt-catalyzed hydrodeoxygenation reactions report a transformation of guaiacol into aromatic products [17,18]. Note that in those cases, lower hydrogen partial pressures and significantly higher temperatures of even 450 °C were applied. Under these conditions, the temperature is high enough to break the C–O bonds directly (without hydrogenation), and hydrogenation of the ring is not favored thermodynamically. However, it should be noted that for a real bio-oil, such high temperatures would lead to immediate cracking and coke formation in the reactor before the catalyst in this work. In this study, a total pressure of 100 bar and low temperatures up to 250 °C were used, which might be the reason for the hydrogenation of the aromatic ring. Furthermore, ring opening might take place at temperatures above 300 °C, especially over zeolite-based catalysts [28].

The results for the conversion of 1-octanol fit well with the results of Gayubo *et al.* [21], who reported the catalytic conversion of various alcohols over H-ZSM-5. Similar to their results, dehydration to octene was achieved here in the first step, while hydrogenation to octane and further hydrocarbons occurred in a second very fast step. In contrast, Mortensen *et al.* [32] reported the decarbonylation of 1-ocatanol to heptanes over Ni-based catalysts, which thus further supports that the main deoxygenation step over zeolite-based catalysts is dehydration.

2.3. Recycling and Regeneration Experiments

For recycling experiments, the catalysts were washed with ethanol and methanol, calcined in air for 10 h at 400 °C and reduced in continuous hydrogen flow. Table 3 compares the initial activity of recycled 1 wt. % Pt/H-MFI-90 with the catalytic activity of the corresponding fresh catalyst and its performance after deactivation. Obviously, the catalytic conversion of guaiacol and 1-octanol could be partly restored leading to a conversion of 35% and 40%, respectively. However, the recycled catalyst deactivated faster than the fresh sample, and the product composition changed with time-on-stream. This behavior is in agreement with the results of Vitolo *et al.* [25], who studied regeneration cycles of H-ZSM-5 and observed a decreasing activity and stability with each regeneration cycle.

Table 3. Comparison of the catalytic performance between fresh and recycled Pt/H-MFI-90 at 250 °C (conditions: 0.3 mL/min 5% GUA in 1-octanol, 500 mL/min 80% H_2/N_2, p = 100 bar, 1.00 g and 0.86 g for the fresh and recycled catalyst).

Pt/H-MFI-90	Time	X_{GUA}	$X_{1\text{-octanol}}$
	(h)	(%)	(%)
Fresh	3	95	96
	6	97	100
	37	10	4
Recycled	3	35	40
	6	13	6

As the catalytic performance was not completely restored after calcination, additional deactivation must have occurred. Both XRD (Figure S1) and STEM analysis (e.g., Figure 1c) of the fresh and used catalysts revealed metal particle sintering and less dispersed particles than before. Furthermore, a decreasing acidity detected by NH_3-temperature programmed desorption (TPD) (Figure S2) and ammonia adsorption (Table 2) of the catalysts, due to calcination during the reactivation might be the reason for the decreased deoxygenation activity (*cf*. [35]). Interestingly, the TPO of the recycled catalyst (Figure 4) showed much lower carbon deposition, thus indicating that less carbonaceous species form due to a loss of acidic sites.

2.4. Influence of the Reaction Temperature and Mechanistic Considerations

To obtain further information on the catalytic performance of 1 wt. % Pt/H-MFI-90, the reaction temperature was decreased stepwise from 250 down to 50 °C using the same catalyst bed (2.5 g). As seen during the stability measurements, deactivation of the catalyst occurred after time-on-stream. To prevent too fast deactivation, a higher amount of catalysts has been used during these temperature studies, and after each new temperature, the system was equilibrated for 3 h. The investigations showed an increased conversion of guaiacol and 1-octanol at a higher temperature with hydrogenation already occurring under milder conditions. At 50 °C, virtually no conversion was observed, whereas full conversion was obtained above 200 °C (Figure 5). For guaiacol, ring hydrogenation was found as the first Pt-catalyzed step, while deoxygenation occurred in a second acid-catalyzed fast step (see Scheme 1). The yield of cyclohexane increased from 0%–88% in a temperature range of 50–200 °C. At 250 °C, methylcyclohexane and methylcyclopentane were formed, whereas the yield of cyclohexane decreased to 49%. Methylcyclohexane and methylcyclopentane appeared in low amounts at 200 °C and increased at 250 °C. During the reaction of guaiacol, methoxycyclohexanol and cyclohexanol were formed as intermediates. At 150 °C, a maximum yield of methoxycyclohexanol (14%) was found, whereas the subsequent reactions to cyclohexanol and cyclohexane were very fast at higher temperatures. At $T > 150$ °C, cyclohexanol was observed only in low amounts (<4%). Under these rather mild reaction conditions, mainly hydrogenation and dehydration occur; for cracking and direct C–O bond cleavage, the temperature is probably too low (*cf*. the discussion in the previous section).

For 1-octanol, hydrodeoxygenation mainly led to octane due to dehydration and hydrogenation (Figure 5; Scheme 1; compare: [21]). In further steps, branched isomers of octane and low amounts of hexanes and pentanes were formed. Hydrogenolysis to heptane, as observed in [32], was hardly found. While virtually no octane was formed at $T \leq 150$ °C, its yield was about 100% at 200 °C, decreasing to 73% at 250 °C. Most probably, octane was cracked into short chain hydrocarbons and octane isomers (16%). Finally, the stability of the catalyst was investigated at 200 and 150 °C over time-on-stream (Figure S3).

Both experiments showed a rather fast deactivation of the catalyst, and the conversion decreased more rapidly than at 250 °C (Figure 3). Probably, at 250 °C, guaiacol might be converted mainly in the first part of the catalyst bed in the beginning of the reaction, and a deactivation zone is assumed to move through the reactor, whereas at lower temperatures, the deactivation can be seen directly from the beginning. Note that carbon deposition after deactivation has been smaller at lower temperatures (Table 2; Figure S4).

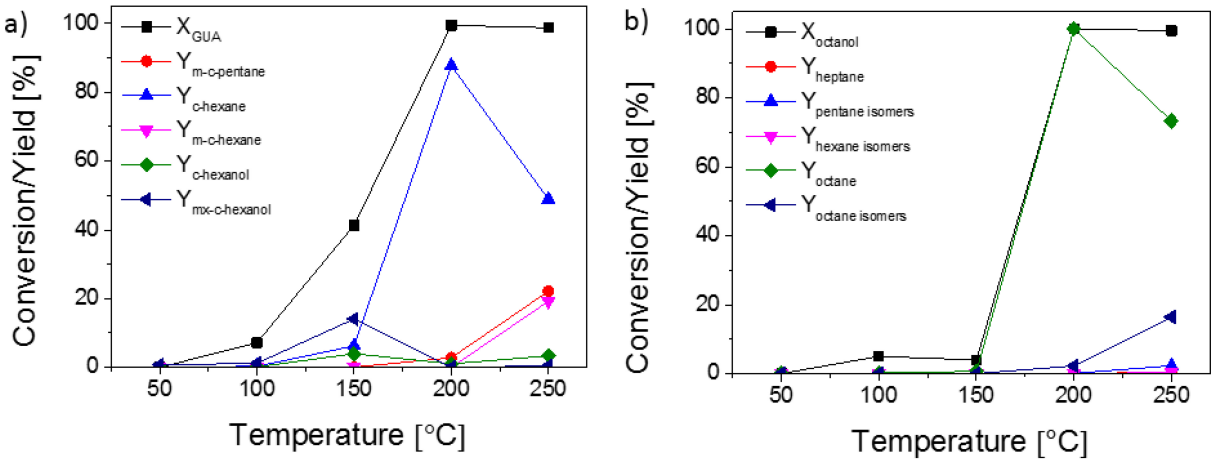

Figure 5. Activity of 1 wt. % Pt/H-MFI-90 in the hydrodeoxygenation of guaiacol (**a**) and 1-octanol (**b**) as a function of the temperature (conditions: 0.3 mL/min 5% GUA in 1-octanol, 500 mL/min 80% H_2/N_2, T = 50–250 °C, p = 100 bar, 2.5 g catalyst; GUA = guaiacol, m = methyl, mx = methoxy, c = cyclo).

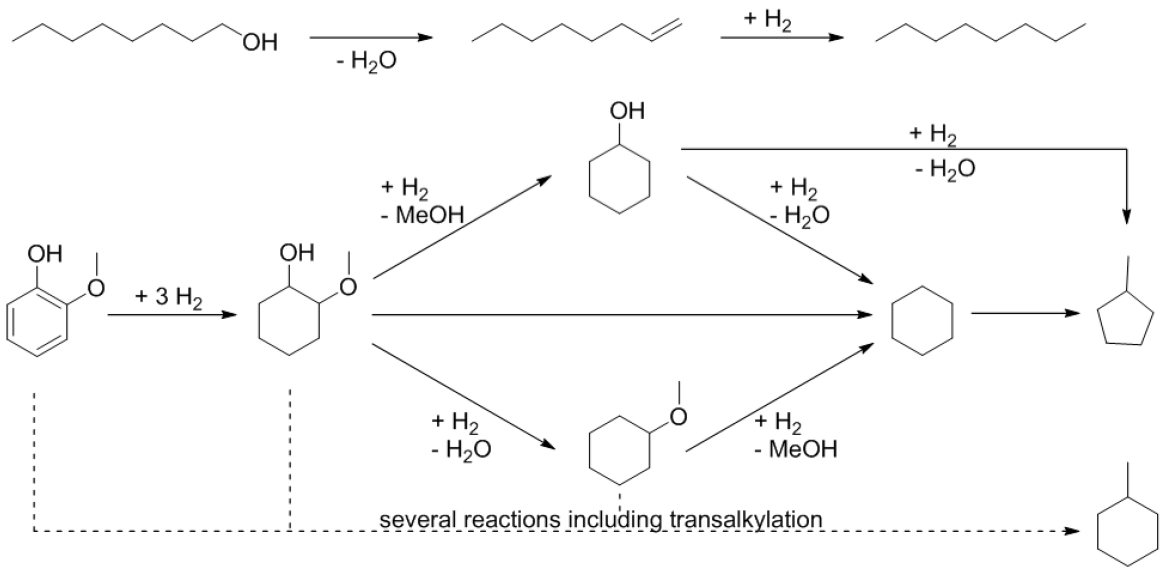

Scheme 1. Reaction pathways for the hydrodeoxygenation of guaiacol and 1-octanol.

3. Materials and Methods

3.1. Catalyst Synthesis

The catalysts were prepared by incipient wetness impregnation to obtain a Pt loading of 1 wt. % and 5 wt. %. Around 15 g of commercially available SiO_2 (Merck, 99%, Darmstadt, Germany) and H-MFI 90 (Clariant, Munich, Germany) were used as supports after drying at 80 °C for 24 h (a higher amount than in a previous study [30] to apply them for continuous operation). The catalysts were prepared by adding an aqueous solution of $Pt(NO_3)_2$ (ChemPur, Karlsruhe, Germany; 1 wt. %: 17.8 $g/g_{support}$, 5 wt. %: 86.7 $g/g_{support}$), so that the total pore volume of the support was filled with the solution (amount of water for SiO_2: 2.96 $g_{H_2O}/g_{support}$; for H-MFI 90: 1.04 $g_{H_2O}/g_{support}$) [36]. The solution was added

dropwise to the support under stirring and dried at 80 °C. Larger amounts were impregnated in several impregnation and drying steps. Finally, the samples were calcined at 400 °C for 2 h (heating rate 100 °C/h). Details on the surface area S_{BET}, acidity and average particle size of the catalysts and the support materials are given in Table 1.

3.2. Catalyst Characterization

The catalysts were characterized by N_2 physisorption, powder X-ray diffraction (XRD), ammonia temperature programmed desorption (NH_3-TPD), temperature programmed oxidation (TPO) and transmission electron microscopy (TEM).

A BELSORP mini II (Rubotherm, Bochum, Germany) was used to measure the specific surface area of the catalysts using the multipoint BET method with N_2 as the adsorbate. The samples were pretreated under vacuum for 2 h at 300 °C.

The acidity of the catalysts was measured in an AutoChem HP Chemisorption Analyzer 2950 (Micromeretics, Norcross, GA, USA) using 0.1 g of catalyst in a U-shaped quartz tube. The samples were pretreated in a continuous flow of He (15 mL/min) for 0.5 h at 400 °C and saturated with ammonia (15 mL/min) at 50 °C. The reactor was heated up to 800 °C (4 K/min) under continuous flow of He (15 mL/min), and the gas mixture was analyzed using a thermal conductivity detector (TCD). The total consumption of NH_3 (not shown) was determined between 50 and 400 °C. Peaks detected below 200 °C were considered as weak and peaks from 200–400 °C as strong acid sites.

XRD patterns were recorded on a PANanalytical X'Pert Pro D8 Advance diffractometer (Almelo, The Netherlands) equipped with a rotating sample holder, a copper anode X-ray source, a nickel filter and a graphite monochromator for Cu Kα (λ = 1.54 Å) radiation. The accelerating voltage and anode current were 40 kV and 45 mA, respectively. The diffraction patterns were measured in Bragg-Brentano geometry in the range 2θ = 20°–80° with a step width of 0.017° and a dwell time of 1 s.

Complementary scanning transmission electron microscopy (STEM) was performed using an FEI Titan 80–300 electron microscope (Hillsboro, OR, USA) operated at 300 kV, and the STEM images were acquired by a Fischione model 3000 HAADF STEM detector (Export, PA, USA) at a magnification of 910 k or higher. The catalyst powder was either crushed or ultrasonically dispersed in ethanol. The crashed powder or one drop of the suspension was brought onto a copper grid covered with holey carbon film, and the suspension was dried in air. The particle size and the particle size distribution analysis was carried out using ImageJ [37].

TPO was performed using a continuous flow reactor. 10-100 mg of the sample were placed in the middle of the reactor. The reactor was heated up to 700 °C at 5 K/min in a mixture of 10% O_2 in N_2 (1000 mL/min). The gases were detected using an AO2020 IR gas analyzer (ABB, Zurich, Switzerland) or an FTIR (MKS instruments, MultiGas™ Analyzer 2030, Andover, MA, USA), respectively.

3.3. Catalytic Measurements

The catalytic tests were performed in a stainless steel continuous fixed-bed flow reactor, described in Ref. [32]. Before the reaction, the catalyst (1.0 g or 2.5 g with a sieve fraction of 300–600 µm;

mixed with glass spheres of a 212–245 μm size to obtain a catalyst bed around 10–11 cm) was pre-treated *in situ* for 1 h in a continuous hydrogen flow (500 mL/min, 10% H_2 in N_2) at atmospheric pressure and 300 °C. The experiment was carried out using a gas mixture of 80% H_2 in N_2 flowing at 500 mL/min and a solution of 5 vol. % guaiacol (GUA, ≥99%, Sigma, St. Louis, MO, USA) in 1-octanol (Sigma, ≥98%) flowing at 0.3 mL/min into the fixed-bed reactor. The reaction temperature was varied between 50 °C and 250 °C at a pressure around 100 bar. At the outlet, the products were separated into gas and liquid products, and the reaction pressure was decreased to atmospheric pressure.

Behind the release valve, gaseous samples were taken every 20–30 min and were analyzed on-line by GC/TCD (Shimadzu GC-2014; Restek, Bellefonte, PA, USA, ShinCarbon ST (SilcoSmooth® Stainless Steel) column, 2 m × 0.53 mm, mesh 80/100). The liquid part was collected over 2 h (also depressurized, cooled to 20 °C). The liquid products were identified and quantified with a GC/MS-FID (Shimadzu GC-MS/FID-QP2010 UltraEi; Sulpelco Equity™ 5 column, Kyoto, Japan, 30 m × 0.32 mm × 0.5 μm).

3.4. Reuse and Reactivation of the Catalyst

After the catalytic measurement, the catalyst was washed 3 times with 4 mL ethanol, as well as 3 times with methanol to remove adhered reaction impurities. To remove the carbon from the previous experiment, the catalyst was treated in air for 10 h at 400 °C. Afterwards, the catalyst was re-reduced in continuous hydrogen flow, as described above.

4. Conclusions

A significant influence of the support on the catalytic conversion, the product distribution and especially the catalyst stability was observed for hydrodeoxygenation of guaiacol and 1-octanol in a continuous process over Pt/SiO_2 and Pt/H-MFI-90. Ring hydrogenation took place in the presence of all catalysts, and acidic sites seemed to be crucial for deoxygenation at low temperature (<250 °C). For the Pt/SiO_2 catalysts, low amounts of deoxygenated products were observed, and the catalysts were stable over longer reaction times. Due to the lack of acidic sites, no conversion of 1-octanol was obtained over the silica-supported catalysts. Using more acidic Pt/H-MFI-90, both guaiacol and 1-octanol were completely converted at temperatures >200 °C. At 200 °C, mainly cyclohexane and octane were formed, while at 250 °C, guaiacol, cyclohexane and octane were partly transformed into methylcyclohexane, methylcyclopentane and octane, respectively. Although this bifunctional catalyst was advantageous for the deoxygenation at T > 250 °C, the acidic support led to a fast deactivation, and at 250 °C, deactivation occurred after 30 h time-on-stream. Reactivation and TPO experiments evidenced that this might be due to coke formation on the catalytic surface. The deactivation may further originate from particle sintering during time-on-stream. Recycling and reactivation experiments resulted only in a partial reactivation. Hence, in future, bifunctional systems that provide medium acidity and, at the same time, a good hydrogenation catalyst activity should be searched for.

Acknowledgments

We thank the Helmholtz Research School "Energy-Related Catalysis", the European Institute of Innovation and Technology under the KIC InnoEnergy project SYNCON, project number 11_2011_IP07_SynCon) and the KIC InnoEnergy PhD program for financial support. We further acknowledge Anders Tiedje and Jakob Munkholt Christensen (Technical University of Denmark), Jan Pesek and Angela Beilmann (Karlsruhe Institute of Technology, KIT) for discussion and help, Clariant (for providing H-MFI) and the Karlsruhe Nano Micro Facility (KNMF, www.kit.edu/knmf) of the Helmholtz Research Infrastructure at KIT (KIT, www.kit.edu) for provision of access to the TEM.

Author Contributions

The experimental work and drafting of the manuscript was carried out by M.H., assisted by S.B., who performed the STEM measurements, and P.M.-M., who built the high pressure setup. W.K. participated in the discussion of the study and the preparation of the manuscript. J.-D.G. and A.D.J. supported the work and cooperation between DTU and KIT, supervised the experimental work, commented on and approved the manuscript. The manuscript was written through the comments and contributions of all authors. All authors have given approval for the final version of the manuscript.

Conflicts of Interest

The authors declare no conflict of interest.

References

1. Torres, W.; Pansare, S.S.; Goodwin, J.G. Hot Gas Removal of Tars, Ammonia, and Hydrogen Sulfide from Biomass Gasification Gas. *Catal. Rev.* **2007**, *49*, 407–456.
2. Mortensen, P.M.; Grunwaldt, J.D.; Jensen, P.A.; Knudsen, K.G.; Jensen, A.D. A review of catalytic upgrading of bio-oil to engine fuels. *Appl. Catal. A* **2011**, *407*, 1–19.
3. Bridgwater, A.V. Production of high grade fuels and chemicals from catalytic pyrolysis of biomass. *Catal. Today* **1996**, *29*, 285–295.
4. Czernik, S.; Bridgwater, A.V. Overview of Applications of Biomass Fast Pyrolysis Oil. *Energy Fuels* **2004**, *18*, 590–598.
5. Venderbosch, R.H.; Ardiyanti, A.R.; Wildschut, J.; Oasmaa, A.; Heeres, H.J. Stabilization of biomass-derived pyrolysis oils. *J. Chem. Technol. Biotechnol.* **2010**, *85*, 674–686.
6. Lin, Y.-C.; Huber, G.W. The critical role of heterogeneous catalysis in lignocellulosic biomass conversion. *Energy Environ. Sci.* **2009**, *2*, 68–80.
7. Huber, G.W.; Iborra, S.; Corma, A. Synthesis of Transportation Fuels from Biomass: Chemistry, Catalysts, and Engineering. *Chem. Rev.* **2006**, *106*, 4044–4098.
8. Ferrari, M.; Bosmans, S.; Maggi, R.; Delmon, B.; Grange, P. CoMo/carbon hydrodeoxygenation catalysts: Influence of the hydrogen sulfide partial pressure and of the sulfidation temperature. *Catal. Today* **2001**, *65*, 257–264.

9. De la Puente, G.; Gil, A.; Pis, J.J.; Grange, P. Effects of Support Surface Chemistry in Hydrodeoxygenation Reactions over CoMo/Activated Carbon Sulfided Catalysts. *Langmuir* **1999**, *15*, 5800–5806.
10. Mortensen, P.M.; Grunwaldt, J.-D.; Jensen, P.A.; Jensen, A.D. Screening of Catalysts for Hydrodeoxygenation of Phenol as a Model Compound for Bio-oil. *ACS Catal.* **2013**, *3*, 1774–1785.
11. He, Z.; Wang, X. Hydrodeoxygenation of model compounds and catalytic systems for pyrolysis bio-oils upgrading. *Catal. Sustain. Energy* **2012**, *1*, 28–52.
12. Foster, A.; Do, P.M.; Lobo, R. The Synergy of the Support Acid Function and the Metal Function in the Catalytic Hydrodeoxygenation of *m*-Cresol. *Top. Catal.* **2012**, *55*, 118–128.
13. Ford, J.; Immer, J.; Lamb, H.H. Palladium Catalysts for Fatty Acid Deoxygenation: Influence of the Support and Fatty Acid Chain Length on Decarboxylation Kinetics. *Top. Catal.* **2012**, *55*, 175–184.
14. Mullen, C.A.; Boateng, A.A.; Reichenbach, S.E. Hydrotreating of fast pyrolysis oils from protein-rich pennycress seed presscake. *Fuel* **2013**, *111*, 797–804.
15. Centeno, A.; Laurent, E.; Delmon, B. Influence of the Support of CoMo Sulfide Catalysts and of the Addition of Potassium and Platinum on the Catalytic Performances for the Hydrodeoxygenation of Carbonyl, Carboxyl, and Guaiacol-Type Molecules. *J. Catal.* **1995**, *154*, 288–298.
16. Laurent, E.; Delmon, B. Study of the hydrodeoxygenation of carbonyl, carboxylic and guaiacyl groups over sulfided CoMo/γ-Al2O3 and NiMo/γ-$Al2O_3$ catalysts: I. Catalytic reaction schemes. *Appl. Catal. A* **1994**, *109*, 77–96.
17. Runnebaum, R.C.; Nimmanwudipong, T.; Block, D.E.; Gates, B.C. Catalytic conversion of compounds representative of lignin-derived bio-oils: A reaction network for guaiacol, anisole, 4-methylanisole, and cyclohexanone conversion catalysed by Pt/γ-Al_2O_3. *Catal. Sci. Technol.* **2012**, *2*, 113–118.
18. Nimmanwudipong, T.; Runnebaum, R.C.; Block, D.E.; Gates, B.C. Catalytic Conversion of Guaiacol Catalyzed by Platinum Supported on Alumina: Reaction Network Including Hydrodeoxygenation Reactions. *Energy Fuels* **2011**, *25*, 3417–3427.
19. Nimmanwudipong, T.; Aydin, C.; Lu, J.; Runnebaum, R.; Brodwater, K.; Browning, N.; Block, D.; Gates, B. Selective Hydrodeoxygenation of Guaiacol Catalyzed by Platinum Supported on Magnesium Oxide. *Catal. Lett.* **2012**, *142*, 1190–1196.
20. Nimmanwudipong, T.; Runnebaum, R.C.; Brodwater, K.; Heelan, J.; Block, D.E.; Gates, B.C. Design of a High-Pressure Flow-Reactor System for Catalytic Hydrodeoxygenation: Guaiacol Conversion Catalyzed by Platinum Supported on MgO. *Energy Fuels* **2014**, *28*, 1090–1096.
21. Gayubo, A.G.; Aguayo, A.T.; Atutxa, A.; Aguado, R.; Bilbao, J. Transformation of Oxygenate Components of Biomass Pyrolysis Oil on a HZSM-5 Zeolite. I. Alcohols and Phenols. *Ind. Eng. Chem. Res.* **2004**, *43*, 2610–2618.
22. Gayubo, A.G.; Aguayo, A.T.; Atutxa, A.; Aguado, R.; Olazar, M.; Bilbao, J. Transformation of Oxygenate Components of Biomass Pyrolysis Oil on a HZSM-5 Zeolite. II. Aldehydes, Ketones, and Acids. *Ind. Eng. Chem. Res.* **2004**, *43*, 2619–2626.

23. Sharma, R.K.; Bakhshi, N.N. Conversion of non-phenolic fraction of biomass-derived pyrolysis oil to hydrocarbon fuels over HZSM-5 using a dual reactor system. *Bioresour. Technol.* **1993**, *45*, 195–203.
24. Pattiya, A.; Titiloye, J.O.; Bridgwater, A.V. Fast pyrolysis of cassava rhizome in the presence of catalysts. *J. Anal. Appl. Pyrolysis* **2008**, *81*, 72–79.
25. Vitolo, S.; Bresci, B.; Seggiani, M.; Gallo, M.G. Catalytic upgrading of pyrolytic oils over HZSM-5 zeolite: Behaviour of the catalyst when used in repeated upgrading–regenerating cycles. *Fuel* **2001**, *80*, 17–26.
26. Murata, K.; Liu, Y.; Inaba, M.; Takahara, I. Hydrocracking of Biomass-Derived Materials into Alkanes in the Presence of Platinum-Based Catalyst and Hydrogen. *Catal. Lett.* **2010**, *140*, 8–13.
27. Murata, K.; Liu, Y.; Inaba, M.; Takahara, I. Production of Synthetic Diesel by Hydrotreatment of Jatropha Oils Using Pt−Re/H-ZSM-5 Catalyst. *Energy Fuels* **2010**, *24*, 2404–2409.
28. Castaño, P.; Gutiérrez, A.; Villanueva, I.; Pawelec, B.; Bilbao, J.; Arandes, J.M. Effect of the support acidity on the aromatic ring-opening of pyrolysis gasoline over Pt/HZSM-5 catalysts. *Catal. Today* **2009**, *143*, 115–119.
29. Ausavasukhi, A.; Huang, Y.; To, A.T.; Sooknoi, T.; Resasco, D.E. Hydrodeoxygenation of *m*-cresol over gallium-modified beta zeolite catalysts. *J. Catal.* **2012**, *290*, 90–100.
30. Hellinger, M.; de Carvalho, H.W.P.; Baier, S.; Wang, D.; Kleist, W.; Grunwaldt, J.-D. Catalytic hydrodeoxygenation of guaiacol over platinum supported on metal oxides and zeolites. *Appl. Catal. A* **2015**, *490*, 181–192.
31. Faglioni, F.; Goddard, W.A. Energetics of hydrogen coverage on group VIII transition metal surfaces and a kinetic model for adsorption/desorption. *J. Chem. Phys.* **2005**, *122*, 014704–014718.
32. Mortensen, P.M.; Gardini, D.; de Carvalho, H.W.P.; Damsgaard, C.D.; Grunwaldt, J.-D.; Jensen, P.A.; Wagner, J.B.; Jensen, A.D. Stability and resistance of nickel catalysts for hydrodeoxygenation: Carbon deposition and effects of sulfur, potassium, and chlorine in the feed. *Catal. Sci. Technol.* **2014**, *4*, 3672–3686.
33. Pham Minh, D.; Gallezot, P.; Besson, M. Treatment of olive oil mill wastewater by catalytic wet air oxidation: 3. Stability of supported ruthenium catalysts during oxidation of model pollutant p-hydroxybenzoic acid in batch and continuous reactors. *Appl. Catal. B* **2007**, *75*, 71–77.
34. Ravenelle, R.; Copeland, J.; Pelt, A.; Crittenden, J.; Sievers, C. Stability of Pt/γ-Al_2O_3 Catalysts in Model Biomass Solutions. *Top. Catal.* **2012**, *55*, 162–174.
35. Zhao, C.; Kasakov, S.; He, J.; Lercher, J.A. Comparison of kinetics, activity and stability of Ni/HZSM-5 and Ni/Al_2O_3-HZSM-5 for phenol hydrodeoxygenation. *J. Catal.* **2012**, *296*, 12–23.
36. Pinna, F. Supported metal catalysts preparation. *Catal. Today* **1998**, *41*, 129–137.
37. Rasband, W.S. ImageJ, U. S. http://imagej.nih.gov/ij/ (accessed on 1 July, 2015).